An X-ray investigation of the NGC 346 field (1) : the LBV HD 5980 and the NGC 346 cluster

Y. Nazé[1,8], J.M. Hartwell[2], I.R. Stevens[2], M. F. Corcoran[3], Y.-H. Chu[4], G. Koenigsberger[5], A.F.J. Moffat[6], and V.S. Niemela[7]

ABSTRACT

We present results from a *Chandra* observation of the NGC 346 star formation region, which contains numerous massive stars, and is related to N66, the largest H II region of the SMC. In this first paper, we will focus on the characteristics of the main objects of the field. The NGC 346 cluster itself shows only relatively faint X-ray emission (with $L_X^{unabs} \sim 1.5 \times 10^{34}$ erg s^{-1}), tightly correlated with the core of the cluster. In the field also lies HD 5980, a LBV star in a binary (or triple system) that is detected for the first time at X-ray energies. The star is X-ray bright, with an unabsorbed luminosity of $L_X^{unabs} \sim 1.7 \times 10^{34}$ erg s^{-1}, but needs to be monitored further to investigate its X-ray variability over a complete orbital cycle. The high X-ray luminosity may be associated either with colliding winds in the binary system or with the 1994 eruption. HD 5980 is surrounded by a region of diffuse X-ray emission, which may be a superimposed supernova remnant.

Subject headings: (galaxies:) Magellanic Clouds–X-rays: individual (NGC 346, HD 5980)

1. Introduction

The Small Magellanic Cloud (SMC) is a an irregular galaxy at a distance of 59 kpc (Mathewson et al. 1986) that forms a pair with the Large Magellanic Cloud (LMC). Both are satellites of our own Galaxy. The interstellar extinction towards the Magellanic Clouds is low, allowing studies of the X-ray sources to be undertaken with only small contamination.

Previous X-ray observations of the SMC have been made with the *Einstein Observatory*, *ASCA* and *ROSAT*. These observations included surveys of the point source population (Kahabka et al. 1999; Schmidtke et al. 1999; Haberl et al. 2000; Sasaki, Haberl, & Pietsch 2000; Yokogawa et al. 2000) and in particular studies of the properties of the X-ray binary population (Haberl & Sasaki 2000). The recent launch of *Chandra*, however, provides the opportunity to study the SMC with a far greater sensitivity and spatial resolution than ever before.

For this investigation of the SMC, the N66 nebula was chosen (Henize 1956). N66 is a giant H II region excited by the NGC 346 cluster, which is the largest star formation area in the SMC.

[1]Institut d'Astrophysique et de Géophysique, Université de Liège, Allée du 6 Août 17, Bat. B5c, B 4000 - Liège (Belgium); naze@astro.ulg.ac.be

[2]School of Physics & Astronomy, University of Birmingham, Edgbaston, Birmingham B15 2TT (UK); jmh@star.sr.bham.ac.uk, irs@star.sr.bham.ac.uk

[3]Universities Space Research Association, High Energy Astrophysics Science Archive Research Center, Goddard Space Flight Center, Greenbelt, MD 20771; corcoran@barnegat.gsfc.nasa.gov

[4]Astronomy Department, University of Illinois, 1002 W. Green Street, Urbana, IL 61801; chu@astro.uiuc.edu

[5]Instituto de Astronomía, Universidad Nacional Autónoma de Mexico, Apdo. Postal 70-264, 04510, Mexico D.F. (Mexico); gloria@astroscu.unam.mx

[6]Département de physique, Université de Montreal, C.P. 6128, Succ. Centre-Ville, Montreal, QC, H3C 3J7 (Canada); moffat@astro.umontreal.ca

[7]Facultad de Ciencias Astronómicas y Geofísicas, Universidad Nacional de la Plata, Paseo del Bosque S/N, B19000FWA La Plata (Argentina); virpi@fcaglp.fcaglp.unlp.edu.ar

[8]Research Fellow F.N.R.S.

This cluster contains numerous massive stars, of spectral type as early as O2 (Walborn et al. 2002). But the large amount of massive stars is not the only feature of interest in this field. On the outskirts of NGC 346 lies the remarkable star HD 5980, which underwent a LBV-type eruption in 1994. This massive binary (or triple?) system was subsequently monitored and analysed for its varying spectral and photometric properties, in visible and UV wavelengths. However, HD 5980 has never been detected by past X-ray observatories. Previous studies of the SMC have discovered a bright extended source along the same line-of-sight as HD 5980 that has been attributed to a SNR. For the SMC, the NGC 346 field thus provides one of the best opportunities to conduct an investigation of the X-ray domain.

In this paper, we will describe in § 2 the observations used in this study, then analyse the available data on NGC 346, HD 5980, and the extended emission in § 3, 4, and 5, respectively. Finally, we will conclude in § 6. The second part of this work (paper II) will describe the properties of the other sources detected in the field.

2. The Observations and Data Analysis

2.1. X-ray observations

NGC 346 was observed with *Chandra* for the XMEGA consortium on 2001 May 15–16 for 100 ks (98.671 ks effective, ObsID = 1881, JD~2 452 045.2d). The data were recorded by the ACIS-I0, I1, I2, I3, S2 and S3 CCD chips maintained at a temperature of -120°C. The data were taken with a frame time of 3.241s in the faint mode. The exposure was centered on the cluster, with HD 5980 lying 1.9′ to the north-east of the aimpoint on ACIS-I3. Our faintest source possess a flux of about 2×10^{32} erg s^{-1} (see paper II), assuming a distance of 59 kpc for the SMC.

We excluded bad pixels from the analysis, using the customary bad pixels file provided by the *Chandra* X-ray Center (CXC) for this particular observation. We have searched the data for background flares, which are known to affect *Chandra* data, by determining the lightcurve of the total count rate, but no flares were found. Event PI values and photon energies were determined using the FITS Embedded File (FEF) acisD2000-01-29fef_piN0001.fits. Note that this calibration matrix is still a preliminary product.

For long exposures, removing the afterglow events can adversely affect the science analysis (underestimation of the fluxes, alteration of the spectra and so on)[9]. We thus computed a new level 2 events file by filtering the level 1 file and keeping the events with *ASCA* grades of 0, 2, 3, 4 and 6, but without applying a status=0 filter. Throughout this paper, we will use this new file for all scientific analysis, except for the source detection, where it is better to use the pipeline level 2 product to avoid mistaking afterglow events for real sources.

Further analysis was performed using the CIAO v2.1.2 software provided by the CXC and also with the FTOOLS tasks. The spectra were analysed and fitted within XSPEC v11.0.1 (Arnaud 1996).

2.2. *HST* WFPC2 images

Two *HST* WFPC2 observations of the N66 / NGC 346 region in Hα are available from the STSci archives. They were taken on 1998 Sept. 27 and 2000 August 7 for the programs 6540 and 8196, respectively. HD 5980 is centered on the PC in the observations from program 6540, while program 8196 shows an area situated further south. The observations were made through the *F656N* filter for 2070s (Prog. # 6540) and 2400s (Prog. # 8196). This filter, centered at 6563.7 Å with a FWHM of 21.4Å, includes the Hα line and the neighboring [N II] lines, but we will neglect here the [N II] contamination.

The calibrated WFPC2 images were produced by the standard *HST* pipeline. We process them further with IRAF and STSDAS routines. The images of each program were combined to remove cosmic rays and to produce a total-exposure map. Apart from HD 5980 (see Fig. 1), no obvious association between X-rays and the Hα emission has been detected in the *HST* data. Fig. 1 will be

[9] see caveat on http://asc.harvard.edu/ciao/caveats/acis_cray.html

discussed more extensively in § 5.

3. The NGC 346 Star Cluster

NGC 346 is the largest star formation region of the SMC. It contains a large fraction of the early O-type stars of this galaxy (Massey, Parker & Garmany 1989). It is related to the giant HII region N66 (Henize 1956), the largest and the most luminous one of the SMC (Ye, Turtle, & Kennicutt 1991). From many points of view, this object constitutes a unique feature in the SMC. The X-ray emission from the cluster itself has never been detected by previous X-ray observatories. Even though part of NGC 346 lies in the ACIS-I CCD gaps, diffuse emission associated with the cluster is seen in the upper corner of ACIS-I3. This position corresponds to the core of the cluster, which contains very early massive stars. In this area, the source detection algorithms found only one source, coincident to the position of star MPG435 (Massey, Parker & Garmany 1989) or N26 (Niemela, Marraco, & Cabanne 1986). However, the emission is not restricted to this star. Most of it correlates well with other bright blue stars, i.e. MPG 368, 396, 417, 470 and 476 (see Fig. 2). But as the X-ray emission of the individual components can not be easily disentangled, we decide to analyse only the overall emission of these sources from now on.

The total count rate of this emission in the $0.3-10.0$ keV band is $3.04 \pm 0.36 \times 10^{-3}$ cnts s^{-1}. If we define S, M and H as the count rates in the $0.3-1.0$ keV, $1.0-2.0$ keV and $2-10.0$ keV energy bands, as in Sarazin, Irwin, & Bergman (2001) and Blanton, Sarazin, & Irwin (2001), we can compute two hardness ratios (HRs), $H21$ and $H31$, defined as $(M-S)/(M+S)$ and $(H-S)/(H+S)$, respectively. The hardness ratios $H21$ and $H31$ of the cluster are 0.41 ± 0.11 and -0.01 ± 0.24, respectively. These ratios are comparable to the softer group of all detected point sources (see paper II).

The spectrum of the NGC 346 cluster was extracted using a carefully chosen background window, as close as possible to the cluster. As we regard the cluster X-ray emission to be extended, we have used the *calcrmf* and *calcarf* tools to generate the appropriate response files. The best fit (χ^2_ν=0.90, N_{dof}=50, $Z = 0.1 Z_\odot$) to this spectrum was an absorbed *mekal* model with the following properties (see Fig. 3): $N(H) = 0.42^{0.83}_{0.17} \times 10^{22}$ cm^{-2} and $kT = 1.01^{2.23}_{0.61}$ keV. The luminosity in the $0.3-10.0$ keV band was 5.5×10^{33} erg s^{-1}, which corresponds to an unabsorbed luminosity of 1.5×10^{34} erg s^{-1}. The hydrogen column is comparable to the value expected for NGC 346 (see paper II), but the temperature is one of the lowest we found, except for the extended source.

In the region of diffuse emission, 30 blue stars have been detected by Massey, Parker & Garmany (1989): MPG 435, 342, 470, 368, 476, 396, 487, 417, 370, 471, 467, 495, 451, 330, 455, 454, 500, 445, 468, 375, 508, 395, 439, 371, 485, 561, 374, 366, 557, 400 (by decreasing magnitude). Of these, 16 have known spectral types that we can use to convert magnitudes to bolometric luminosities. The bolometric correction factors were taken from Humphreys & McElroy (1984). We can then predict the expected X-ray luminosities using $log(L_X^{unabs}) = 1.13 \log(L_{BOL}) - 11.89$ (Berghöfer et al. 1997). If the X-rays were coming only from these 16 stars, we should expect a total unabsorbed luminosity of 2×10^{33} erg s^{-1}. This represents only 13% of the detected luminosity. Several hypotheses could explain this discrepancy: a metallicity effect (Berghöfer's relation was determined for Galactic stars), X-ray emission from the other (unclassified) stars in this region, additional emission linked to interactions in binary systems (such as colliding winds), emission from wind-blown bubble(s) around star(s) of the cluster core, or an extended region of hot gas as the winds from the individual stars combine to form a cluster wind (Cantó, Raga, & Rodríguez 2000).

Chandra has also observed X-ray emission from other very young (age < 5 Myr) stellar clusters, comparable to NGC 346. The Arches clusters in the Galactic Center region has been observed to have emission from several different regions, with a total X-ray luminosity of $L_X^{unabs} \sim 4 \times 10^{35}$ erg s^{-1} (Yusef-Zadeh et al. 2002). NGC 3603 has also been observed with *Chandra* (Moffat et al. 2002)

and the total unabsorbed cluster luminosity is $L_X^{unabs} \sim 1 \times 10^{35}$ erg s^{-1} (though in this case it is clear that a substantial fraction of the emission is from point sources in the cluster). For both the Arches and NGC 3603 clusters the fitted temperature of the X-ray emission is higher than the $kT \sim 1$ keV value for NGC 346.

It is worth noting that both the NGC 3603 and Arches clusters are probably a little more massive than NGC 346 (comparing the estimated number of ionizing photons quoted for NGC 346 by Massey, Parker & Garmany (1989) and for NGC 3603 and the Arches by Figer, McLean, & Morris (1999)), and presumably the total mass and energy injection by the stars in the NGC 346 cluster is correspondingly only somewhat smaller. NGC 346 is rather less luminous than both NGC 3603 and the Arches. This degree of variation is somewhat surprising as, on theoretical grounds, we would expect the cluster X-ray luminosity to scale as $\dot{M}_{cl}^2$, with $\dot{M}_{cl}$ the integrated mass-loss rate from the stars in the cluster (Cantó, Raga, & Rodríguez 2000), which we might expect to be broadly similar. It is perhaps worth noting that in the case of NGC 346, because of the detector orientation and the lower flux levels, it could be that we are underestimating the cluster luminosity.

4. The LBV HD 5980

If NGC 346 contains a large fraction of the massive stars of the SMC, at least one of the stars in this field, HD 5980, is certainly unique in itself and worth further examination. This eclipsing binary (or triple system?) was classified as WN+OB before 1980, but its spectral type changed to WN3+WN4 in 1980–1983, and to WN6, with no trace of the companion, in 1992. In 1994, this star underwent a LBV-type eruption, and presented at the same time a WN11 type. The eruption has now settled down and the values are coming back to the pre-eruption ones (for more details see Koenigsberger et al. (2000) and references therein).

Chandra is the first X-ray telescope to detect this peculiar system. However, even with a 100 ks exposure, the data possess a rather low signal-to-noise ratio. HD 5980 has a count rate of only $2.98 \pm 0.19 \times 10^{-3}$ cnts s^{-1} in the $0.3 - 10.0$ keV band and a hardness ratio ($H21$, $H31$) of (0.43, 0.34), a rather low value compared to the other detected point sources (see paper II).

We have extracted a spectrum of HD 5980 using the CIAO tool *psextract*. An annular background region around the source was chosen, in order to eliminate contamination from the surrounding extended emission (see § 5). This spectrum is shown in Fig. 4a. The best fit model to the data has the following parameters: $N(H) = 0.22^{0.14}_{0.35} \times 10^{22}$ cm^{-2} and $kT = 7.04^{4.35}_{13.35}$ keV for an absorbed *mekal* model and $N(H) = 0.28^{0.19}_{0.44} \times 10^{22}$ cm^{-2} and Γ=$1.74^{1.53}_{1.89}$ for an absorbed power-law. These hydrogen columns are consistent with the value expected for NGC 346 (see paper II). The derived absorbed X-ray luminosity of HD 5980 is $L_X = 1.3 \times 10^{34}$ erg s^{-1} in the $0.3 - 10.0$ keV band for both models. Using the normalisation factor of the mekal model, we found a volume emission measure of $\sim 10^{57}$ cm^{-3} for this star.

We can try to compare HD 5980 with other WR stars detected in X-rays. The unabsorbed X-ray luminosity of HD 5980 is 1.7×10^{34} erg s^{-1} in the $0.3 - 10.0$ keV energy range and 9×10^{33} erg s^{-1} in the *ROSAT* range, i.e. $0.2 - 2.4$ keV. This places HD 5980 amongst the most X-ray bright single WN stars (Wessolowski 1996) and the brightest WR+OB binaries (Pollock 2002) of the Galaxy.

Two factors could explain this high X-ray luminosity. First, the fast wind from the post-eruptive phases (from 1300 km s^{-1} in 1994 to $\sim$2000 km s^{-1} in 2000) should now collide with the slow wind (ejected with a velocity as low as 200 km s^{-1} during the eruption), which will increase the post-eruptive X-ray luminosity. X-ray emission from colliding ejecta has already been observed for another LBV, i.e. η Carinae. Close to this star, the detected X-ray emission is correlated to the high velocity ejecta of the Homunculus nebula (Weis, Duschl, & Bomans 2001), which was created after the last great eruption. For HD 5980, however, the ejecta from the 1994 eruption has not had sufficient time enough to form a detectable LBV nebula around the star, and no 'Homunculus-like' nebula from a previous eruption

is visible around HD 5980 (see Fig. 1): any X-ray emission from the colliding ejecta should thus still be blended with the stellar emission from HD 5980 and that may contribute to explain the high X-ray luminosity. Unfortunately, no X-ray observation of HD 5980 before the 1994 eruption is available, which would allow us to quantitatively compare the pre- and post-eruption luminosities and confirm this predicted luminosity enhancement.

The fact that HD 5980 is a close binary system, containing two very massive stars suggests that colliding winds may provide another source for the observed X-rays, and we can make an estimate of the expected X-ray luminosity in this case. For the system, we assume that the stellar winds of the stars have returned to their pre-eruption values and we assume that $\dot{M}_A$=1.4$\times$ 10^{-5} $M_\odot$ yr^{-1}, $v_\infty(A)$=2500 km s^{-1} for the O-star, and $\dot{M}_B$=2$\times 10^{-5}$ $M_\odot$ yr^{-1}, $v_\infty(B)$=1700 km s^{-1} for the WN Wolf-Rayet star (Moffat et al. 1998). Thus the momenta of each stars wind are very similar, and the total wind kinetic energy is 5×10^{37} erg s$-$1. These wind parameters lead to a momentum ratio of $\eta = 0.97$ (Usov 1992) and the wind-wind collision shock will lie halfway between the stars. In this configuration we expect about 1/6 of the wind kinetic energy to pass perpendicularly through the two shocks and be thermalised (Stevens, Blondin, & Pollock 1992), and because the systems are relatively close much of this energy will be radiated[10].

Consequently, we would expect the X-ray luminosity of HD 5980 to be $\sim 10^{36}$ erg s^{-1} or more, rather than the observed value of $\sim 10^{34}$ erg s^{-1}. The discrepancy between the predicted and observed X-ray luminosities could be due to a range of factors, e.g. the winds may not be at the pre-eruption levels - lower mass-loss rates or lower wind velocities will translate to a lower X-ray luminosity. Alternatively, the wind momenta may not be nearly equal, as a low value of η also tends to lower the luminosity.

Using the ephemeris of Sterken & Breysacher (1997), we have computed a phase of ϕ = 0.24 $-$ 0.30 for our *Chandra* observation: this is close to the eclipse of star A (which is the 1994 eruptor), by star B (ϕ=0.36). If the eccentricity is $e \sim 0.3$ a simple adiabatic model predicts that the X-ray luminosity will vary inversely with separation and so we might expect a change in the intrinsic X-ray luminosity of ~ 2 through the orbit and of $\sim$ 10% during the *Chandra* observation. We have detected a variation of apparently larger amplitude in the count rate of HD 5980 (see Fig. 4b). This still suggests we are seeing orbital variability associated with colliding winds, since the additional effects of changing absorption on the observed luminosity can either reduce or enhance this variability. This observed variability is much more likely to be due to colliding winds than wind-blown bubble type emission, where no short timescale variability would be expected. The high fitted temperature of HD 5980 $kT \sim$ 7keV also suggests that we are likely seeing colliding wind emission, as this temperature corresponds to a pre-shock velocity of $\sim$ 2500 km s^{-1}, comparable to that anticipated.

However, the detailed characteristics of the X-ray properties of HD 5980 need to be studied further, in conjunction with detailed colliding wind models (c.f. the case of η Carinae; Pittard & Corcoran 2002). An *XMM-Newton* observation is scheduled at phases ϕ = 0.09 $-$ 0.10, just after periastron: the comparison between both datasets may enable us to detect further the signature of the colliding wing region, and constrain it more precisely.

Finally, we may note that the unabsorbed X-ray luminosity of the central source in η Carinae, if we assume a distance of 2.3 kpc, varies between 0.6 and 2.5$\times 10^{35}$ erg s^{-1} (Ishibashi et al. 1999), which is much lower than HD 5980.

5. The Extended Emission around HD 5980

Around the position of HD 5980 lies a region of X-ray bright extended emission. It was first detected by the *Einstein Observatory* (source IKT 18 in Inoue, Koyama, & Tanaka (1983)), and subsequently observed by *ROSAT* (source [HFP2000]

[10]In terms of the cooling parameter χ defined by Stevens, Blondin, & Pollock (1992), for the WN wind $\chi \ll 1$ and for the O-star wind $\chi \sim 1$.

148[11] in Haberl et al. (2000)). The overall shape of the emission is more or less rectangular, with an extension to the northeast. It contains a few bright or dark arcs, but apart from these, the brightness is rather uniform, with no obvious limb-brightening. It has a size of $130'' \times 100''$, i.e. 37pc×29pc at the SMC's distance. HD 5980 lies towards the top center of the source. An X-ray bright filament extends from $9''$ west of the star to $23''$ to its south. An X-ray dark feature appears some $30''$ at the southeast of HD 5980. The total count rate of this source in the 0.3 – 10.0 keV energy range is $7.25 \pm 0.17 \times 10^{-2}$ cnts s^{-1}, and the hardness ratios $H21$ and $H31$ are -0.24 ± 0.02 and -0.96 ± 0.05, respectively: it is the only soft source present in the field.

The spectrum of the extended emission was extracted with a carefully chosen background region, located as close as possible to the source and in a region on the ACIS-I1 CCD where there are no point sources. As the X-ray emission is extended the rmf and arf matrices were calculated using the *calcrmf* and *calcarf* tools. The best fit (χ^2_ν=1.03, N_{dof}=244) to this spectrum was an absorbed *mekal* model with the following properties (see Fig. 5): $N(H) = 0.12^{0.15}_{0.10} \times 10^{22}$ cm^{-2}, $kT = 0.66^{0.68}_{0.64}$ keV and $Z = 0.17^{0.21}_{0.15} Z_\odot$. The flux in the 0.3 – 10.0 keV band was 3.35×10^{-13} erg cm^{-2} s^{-1}, i.e. a luminosity of 1.40×10^{35} erg s^{-1}. The low value of the hydrogen column suggests that this X-ray source lies between NGC 346 and the observer, but still in the SMC (see paper II). The hydrogen column is, however, larger than the value predicted using ultraviolet absorptions (Koenigsberger et al. 2001; Hoopes et al. 2001).

Using the normalisation factor of the mekal model, we found a volume emission measure $\int n_e n_H dV$ of $\sim 3 \times 10^{58}$ cm^{-3}. Considering a constant density for the hot gas, a sperical geometry of diameter ~33 pc for the extended emission and assuming a pure H composition, the density of the hot gas is roughly 0.2 cm^{-3} and the total mass of the hot gas is ~100 $M_\odot$.

Using the available data, a deeper analysis was conducted, searching for the existence of a temperature gradient throughout the source area, with color and temperature maps. For color maps, we generated a set of narrow-band images, e.g. 0.3 – 0.9 keV, 0.9 – 1.2 keV and 1.2 – 2.0 keV, that enables us to distinguish the harder components from the softer parts. In addition, temperature maps were constructed from spectral fits in small regions of the SNR. The only obvious trend in both the color and temperature maps is the softness of the northeastern extension of the SNR. However, it is not possible to draw any firm conclusions regarding the presence of any temperature gradient.

We have also constructed images of the extended emission in narrow wavelength bands, each corresponding to a specific ion. The data in each band were first binned to obtain $4.9'' \times 4.9''$ pixels, and then smoothed by convolution with a Gaussian of σ = 0.5 pixel (see Fig. 6). In contrast to N132D (Behar et al. 2001), no significative differences between the morphology of highly ionized species (Mg^{10+}, Ne^{9+}, Si^{12+}, Fe^{19+}) and lower ionization species were detected.

5.1. The Nature of the Extended Emission

Since its discovery the extended X-ray emission has been attributed to a supernova remnant (SNR). Further evidence was subsequently obtained to support this hypothesis; for example, Ye, Turtle, & Kennicutt (1991) found a non-thermal radio source at this position thay they called SNR 0057 – 7226. Using the lowest contours of Ye, Turtle, & Kennicutt (1991), the radio source is 56 pc×52 pc, slightly larger than the X-ray source.

Moreover, evidence of high velocity motions in this region were observed in the visible and UV ranges. Using echelle spectra centered on Hα, Chu & Kennicutt (1988) found clumps moving at +170 km s^{-1} from the main quiescent component ($v_{LSR} \sim 300$ km s^{-1}): only the receding side of the expanding object is seen, suggesting a low density where the approaching side arises. UV analyses with *IUE* (de Boer & Savage 1980), *HST* STIS (Koenigsberger et al. 2001) and *FUSE* (Hoopes et al. 2001) have also confirmed the presence of an expanding structure. But while de Boer

[11]This *ROSAT* source may encompass some of the X-ray emission from the cluster.

& Savage (1980) and Hoopes et al. (2001) found only absorptions at v_{LSR}=+300 km s^{-1}, Koenigsberger et al. (2001) detected both expanding sides of the object, with components at v_{LSR} = +21, +52, +300, +331 km s^{-1}. However, the absorptions at +21 and +52 km s^{-1} were small, and needed a future confirmation (Koenigsberger, private communication). Absorptions at any of these velocities are not seen in the spectra of Sk 80, a close neighbor of HD 5980 situated on the edge of the X-ray source. A fast expanding structure close to the position of HD 5980 is thus present.

Unfortunately, even the high-resolution *HST* WFPC2 images of the close neighborhood of HD 5980 do not show any clear nebula associated with this object (see Fig. 1). However, a lot of filamentary structures - generally indicative of a SNR (Chen et al. 2000) - are seen throughout the field, but are not limited to the exact location of the X-ray source. There is thus no obvious Hα feature directly associated with the extended emission.

Considering all the evidence (non-thermal emission, high velocity expanding shell etc), the X-ray / radio source should thus be regarded as a SNR located in front of HD 5980 but still belonging to the SMC. The SNR hypothesis is further supported by the comparison of the size of this feature to its X-ray and radio fluxes (Mathewson et al. 1983).

However, as HD 5980 is projected more or less in the middle of this X-ray emission, it is hard to believe that there is no link at all between the two and that we have here only a chance superposition, especially when we know that HD 5980 has undergone a LBV-type eruption in 1994. This 1994 eruption is unlikely to be the only one undergone by the system. Can we find any evidence showing that HD 5980 is directly responsible for this emission?

First of all, we can compare HD 5980 with other objects, since there are known interactions of other LBVs with their surroundings, e.g. η Carinae, the most famous LBV of the sky. This star is indeed surrounded by an X-ray bright extended emission associated with the entire Carina Nebula: it is comparable in X-ray temperature (kT), size and morphology to the X-ray emission around HD 5980 (Seward & Mitchell 1981 ; Fig.7). But it is generally assumed that this Nebula has been formed through the collective action of all stars of the Carina cluster, not only by the single action of η Carinae. Also, the expansion velocity of the Carina Nebula is far smaller than ours: 15–20 km s^{-1}, see Walborn & Hesser (1975). All high velocity structures in this nebula are smaller structures localized closely on a few stars.

However, Walborn (1978) claimed to have found some evidence of interaction between HD 5980 and its surroundings: an arc of radius $\sim 30''$ centered on the star is actually visible in Hα and [O III] (but not in [S II]). But this arc is rather diffuse (see Fig. 1), indicating a lack of shock compression. Moreover, its velocity is the one of the quiescent region, and no splitting region is seen beginning at the arc and extending towards the star: this arc is certainly not the rim of an expanding shell. Finally, no strong correlation with the X-ray bright arc can be derived: both have different sizes and shapes, as can be appreciated on Fig. 1, and we can therefore conclude that they probably belong to two distinct features. The comparison between X-rays and visible data thus do not show any clear indication of an interaction between HD 5980 and its environment.

Other clues also seem to reject such a possibility. For an interaction between a LBV nebula and circumstellar material surrounding the star, we should detect an enhancement of the [N II]/Hα ratio, like for SNR 0540 – 69.3 in the LMC, SNR 0102 – 72.3 in the SMC or the ultra-luminous SNR in NGC 6946 (Dunne, Gruendl, & Chu 2000): this is not seen in the echelle spectra of this area and we have therefore to reject this possibility. We also note that none of these interactions could explain the redshifted UV absorptions in the spectra of HD 5980, nor the non-thermal radio emission from the extended source.

The final possibility is that the source is indeed a SNR, but that HD 5980 is still directly responsible for it. The third component of this system could be a compact object, a remnant of

the star that exploded as a SN long ago. However, as the SNR is now in front of HD 5980 (as indicated by the UV absorptions and the low hydrogen column), HD 5980 should have been ejected and have velocity of $> +300\,\mathrm{km\,s^{-1}}$. Unfortunately, Koenigsberger et al. (2000) show that the average velocity of the system is entirely compatible with that of the NGC 346 cluster (but this conclusion only applies to the radial component, since nothing is known on the tangential motion of the star). Therefore we conclude that, most probably, another very massive star from the NGC 346 field - whose stellar remnant has never been detected up to now - is the probable progenitor of the SN explosion.

6. Summary

In this serie of articles, we report the analysis of the *Chandra* data of NGC 346, the largest star formation region of the SMC. In this first paper, we have focused on the most important objects of the field : the NGC 346 cluster and HD 5980.

The cluster itself was relatively faint, with a total luminosity of $L_X^{unabs} \sim 1.5 \times 10^{34}$ erg s^{-1}. Most of this emission seems correlated with the location of the brightest stars of the core of the cluster, but the level of X-ray emission probably cannot be explained solely by the emission from individual stars.

In this field lies another object of interest: HD 5980, a remarkable star that underwent a LBV-type eruption in 1994. *Chandra* is in fact the first X-ray telescope to detect HD 5980 individually. In X-rays, the star appears very bright, comparable only to the brightest WR stars in the Galaxy. The comparison of our results with future X-ray observations will enable us to better understand HD 5980: for example, phase-lock variations would be analysed in the perspective of the colliding wind behaviour of this binary, while other variations may be related to the recent LBV eruption. Follow-up observations are thus needed to complete the study of this system.

A bright, extended X-ray emission is seen to surround this star, but it is probably due to a SNR unrelated to the star, the progenitor of which is unknown. We note however its close resemblance to the Carina Nebula in which the LBV η Carinae lies.

REFERENCES

Arnaud, K. 1996, ASP Conf. Ser. 101, eds G. Jacoby & J. Barnes, p.17

Behar, E., Rasmussen, A.P., Griffiths, R.G., Dennerl, K., Audard, M., Aschenbach, B., & Brinkman, A.C. 2001, A&A, 365, L242

Berghöfer, T.W., Schmitt, J.H.M.M., Danner, R., & Cassinelli, J.P. 1997, A&A, 322, 167

Blanton, E.L., Sarazin, C.L., & Irwin, J.A. 2001 ApJ, 552, 106

Cantó, J., Raga, A.C., & Rodríguez, L.F. 2000, ApJ, 536, 896

Chen, C.-H. R., Chu, Y.-H., Gruendl, R.A., & Points, S.D. 2000, AJ, 119, 1317

Chu, Y.-H., & Kennicutt, R.C., Jr 1988, AJ, 95, 1111

de Boer, K.S., & Savage, B.D. 1980, ApJ, 238, 86

Dunne, B.C., Gruendl, R.A., & Chu, Y.-H. 2000, AJ, 119, 1172

Figer, D.F., McLean, I.S., Morris, M., 1999, ApJ, 514, 202

Haberl, F., Filipovic, M. D., Pietsch, W., & Kahabka, P. 2000, A&AS, 142, 41 (HFP2000)

Haberl, F., & Sasaki, M. 2000, A&A 359, 573

Henize, K.G. 1956, ApJS, 2, 315

Hoopes, C.G., Sembach, K.R., Howk, J.C., & Blair, W.P. 2001, ApJ, 558, L35

Humphreys, R.M. & McElroy, D.B. 1984, ApJ, 284, 565

Inoue, H., Koyama, K., & Tanaka, Y. 1983, IAUS, 101, 535 (IKT)

Ishibashi, K., Corcoran, M.F., Davidson, K., Swank, J.H., Petre, R., Drake, S.A., Damineli, A., & White, S. 1999, ApJ, 524, 983

Kahabka, P., Pietsch, W., Filipovic, M. D., & Haberl, F. 1999, A&AS, 136, 81

Koenigsberger, G., Georgiev, L., Barbà, R., Tzvetanov, Z., Walborn, N.R., Niemela, V.S., Morrell, N., & Schulte-Ladbeck, R. 2000, ApJ, 542, 428

Koenigsberger, G., Georgiev, L., Peimbert, M., Walborn, N.R., Barbà, R., Niemela, V.S., Morrell, N., Tsvetanov, Z., & Schulte-Ladbeck, R. 2001, AJ, 121, 267

Massey, P., Parker, J.W., & Garmany, C.D. 1989, AJ, 98, 1305

Mathewson, D.S., Ford, V.L., Dopita, M.,A., Tuohy, I.R., Long, K.S., & Helfand, D.J. 1983, ApJS, 51, 345

Mathewson, D.S., Ford, V.L., & Visvanathan, N. 1986, ApJ 301, 664

Moffat, A.F.J., Marchenko, S.V., Bartzakos, P., Niemela, V.S., Cerruti, M.A., Magalhaes, A.M., Balona, L., St-Louis, N., Seggewiss, W., & Lamontagne, R. 1998, ApJ, 497, 896

Moffat, A.F.J., et al., 2002, ApJ, (in press)

Niemela, V.S., Marraco, H.G., & Cabanne, M.L. 1986, PASP, 98, 1133

Pittard, J.M., & Corcoran, M.F. 2002, A&A, 383, 636

Pollock, A.M.T. 2002, Interacting winds from massive stars, eds A.F.J. Moffat & N. St Louis, ASP Conf. Series, p 363

Sarazin, C.L., Irwin, J.A., & Bergman, J.N. 2001, ApJ, 556, 533

Sasaki, M., Haberl, F., & Pietsch, W. 2000, A&AS, 147, 75

Schmidtke, P.C., Cowley, A.P., Crane, J.D., Taylor, V.A., McGrath, T.K., Hutchings, J.B., & Crampton, D. 1999, AJ, 117, 927

Seward, F.D. & Mitchell, M. 1981, ApJ, 243, 736

Sterken, C. & Breysacher, J. 1997, A&A, 328, 269

Stevens I.R., Blondin J.M., Pollock, A.M.T. 1992, ApJ, 386, 265

Usov, V.V. 1992, ApJ, 389, 635

Walborn, N.R. & Hesser, J.E. 1975, ApJ, 199, 535

Walborn, N.R. 1978, ApJ, 224, L133

Walborn, N.R., Howarth, I.D., Lennon, D.J., Massey, P., Oey, M.S., Moffat, A.F.J., Skalkowski, G., Morrell, N.I., Drissen, L., & Parker, J.W. 2002, AJ, in press

Weis, K., Duschl, W.J., & Bomans, D.J. 2001, A&A, 367, 566

Wessolowski, U. 1996, MPE report No. 263, 75

Ye, T., Turtle, A.J., & Kennicutt, R.C., Jr. 1991, MNRAS, 249, 722

Yokogawa, J., Imanishi, K., Tsujimoto, M., Nishiuchi, M., Koyama, K., Nagase, F., & Corbet, R.H.D. 2000, ApJS, 128, 491

Yusef-Zadeh, F., Law, C., Wardle, W., Wang, Q.D., Fruscione, A., Lang, C.C., Cotera A. 2002, ApJ, (in press)

This 2-column preprint was prepared with the AAS LaTeX macros v5.0.

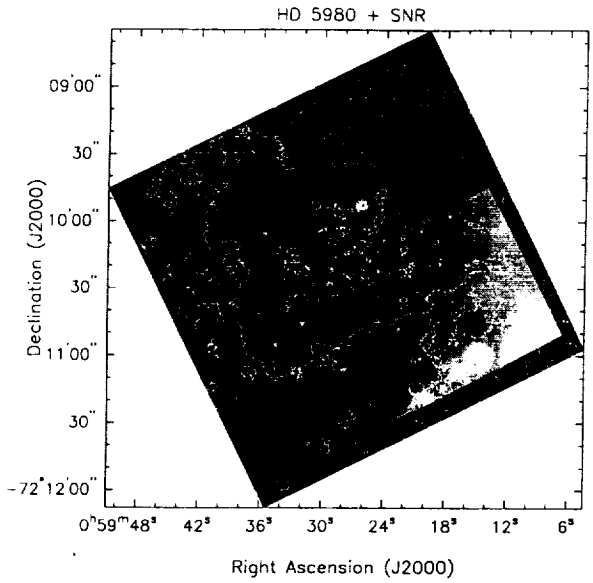

Fig. 1.— *HST* WFPC2 Hα data of the region surrounding HD 5980 (which is the star located at the center of the PC chip), with the adaptively smoothed *Chandra* X-ray data overlaid as contours. The extended X-ray emission and the X-ray emission associated with HD 5980 are clearly seen. Parts of the NGC 346 cluster are visible in the SW portion of the field.

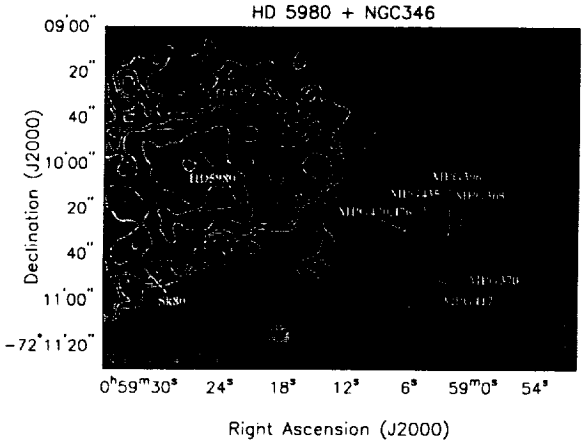

Fig. 2.— The smoothed *Chandra* X-ray data of the NGC 346/HD 5980 region (smoothing by convolution with a gaussian of $\sigma = 2.5''$) superimposed on the *DSS* image, showing the extended nature of the X-ray source associated with the cluster. The location of the brightest stars in the cluster are indicated.

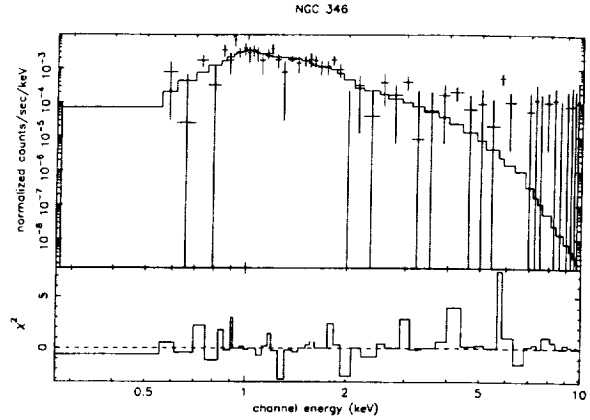

Fig. 3.— The X-ray spectrum of the NGC 346 cluster (Src 36), shown along with the best-fit absorbed *mekal* model, with $N(H) = 0.42 \times 10^{22}$ cm^{-2} and $kT = 1.01$ keV (see § 3).

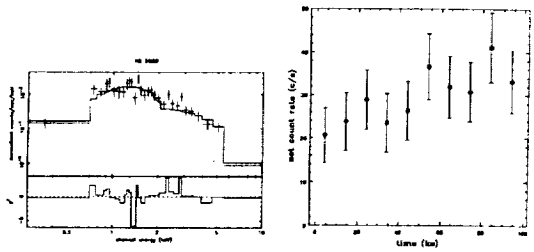

Fig. 4.— a. The *Chandra* X-ray spectrum of HD 5980, shown along with the best-fit absorbed *mekal* model, with $N(H) = 0.22 \times 10^{22}$ cm^{-2} and $kT = 7.04$ keV. b. The *Chandra* X-ray lightcurve of HD 5980, in the 0.3-10 keV range and with 10 bins of 10 ks each.

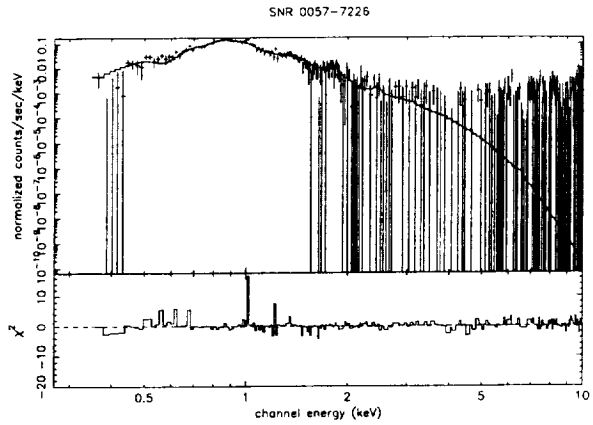

Fig. 5.— The *Chandra* X-ray spectrum of the extended emission around HD 5980, shown along with the best-fit absorbed *mekal* model, with $N(H) = 0.12 \times 10^{22}$ cm^{-2}, $kT = 0.66$ keV and $Z = 0.17 Z_{\odot}$ (see § 5).

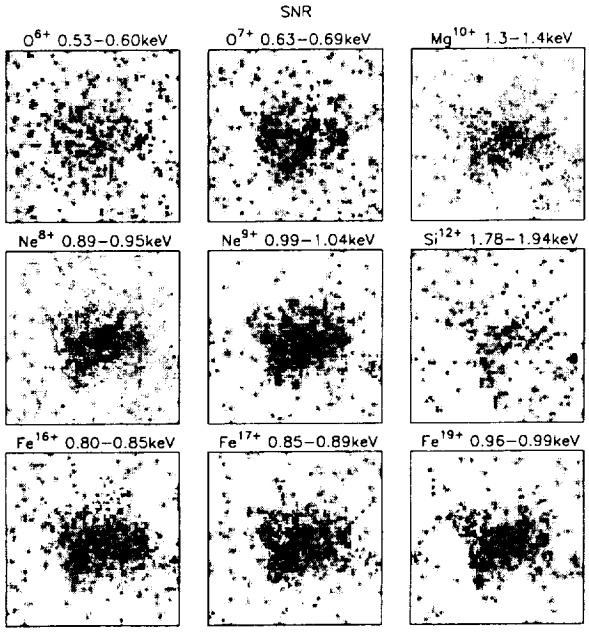

Fig. 6.— Narrow-band images of the extended emission surrounding HD 5980. Each image is labeled with the principal line-emitting ion and the energy range used to generate the image.

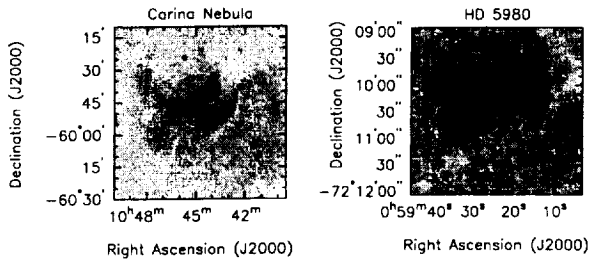

Fig. 7.— The Carina Nebula compared to the extended emission around HD 5980. If we assume a distance of 2.3 kpc for the Carina Nebula and 59 kpc for the SMC, both images are ~55 pc×55 pc. ROSAT PSPC support rings and *Chandra* ACIS-I CCD gaps can be spotted on these images. Both images were smoothed by convolution with a gaussian (σ=2.5″ for HD 5980 and 15″ for the Carina Nebula).